ELSEVIER

Journal of Fluids and Structures 20 (2005) 1057–1071

JOURNAL OF FLUIDS AND STRUCTURES

www.elsevier.com/locate/jfs

Characteristic time scales of velocity and pressure events

C.C. Chabalko[a], D.A. Jordan[b], M.R. Hajj[a,*], H.W. Tieleman[a]

[a]*Department of Engineering Science and Mechanics, Virginia Tech, Blacksburg, VA 24061, USA*
[b]*Department of Mechanical and Aerospace Engineering, University of Virginia Charlottesville, VA 22904, USA*

Received 8 October 2003; accepted 3 May 2005
Available online 27 June 2005

Abstract

Numerical and wind tunnel simulations of full-scale wind loads on structures are usually performed at a lower Reynolds number and different turbulence parameters. One way to assess the validity of such simulations is through matching magnitudes, duration and/or spectral characteristics of simulated pressure peaks with full-scale data. Because wavelet analysis provides a time/frequency decomposition, it has been proposed as an analysis tool for the intermittent and transient pressure peaks. This work aims at answering the question as to whether different wavelets yield the same-scale decomposition of pressure peaks and velocity events and could, thus, be used as a tool for the analysis of extreme loads on structures. The results show that, by isolating the peaks or events with a modified Gaussian window prior to applying the wavelet transform, the dependence of the measured time scale on different wavelet functions is reduced. The time scales of the pressure peak and the velocity event are estimated to be about the same indicating that one contributing factor, at the peak scale, to the pressure peak lies in the variation of the incoming flow at the same scale.

Keywords: Morlet wavelet; Paul wavelet; Time scales; Wind loads; Pressure peaks

1. Introduction

Wind tunnel and numerical simulations of full-scale experiments of wind loads on low-rise structures require similarity of the Reynolds number as well as the turbulence level in the incident flow. Unfortunately, because the full-scale Reynolds number is about 10^7, its dynamic similarity is not achievable in wind tunnel simulations. Additionally, matching all turbulence parameters such as turbulence intensities, integral length scales, small-scale parameters and aerodynamic roughness lengths has been shown to be extremely difficult. The major reason is that all of these parameters could not be varied independently. Added to these issues is the fact that, while wind tunnel and numerical simulations can be repeated many times and runs can be made over long periods of time, full-scale measurements are usually made over relatively shorter durations. All of these difficulties raise several questions among which are the following: on what basis should simulated and full-scale measured wind loads be compared? Should this basis be the level of pressure peak, its duration, and/or its probability of non-exceedence? Should it be the spectral characteristics of the time series of the pressure coefficients? Should it be based on the relation between the flow field and the surface pressures?

*Corresponding author. Tel.: +1 540 231 4190; fax: +1 540 231 4574.
E-mail address: mhajj@vt.edu (M.R. Hajj).

0889-9746/$ - see front matter
doi:10.1016/j.jfluidstructs.2005.05.002

Answers to the above questions are important from different perspectives. For instance, while matching peak levels is important for prediction of extreme static loads, matching other parameters such as duration or spectral characteristics of pressure fluctuations is of interest when considering dynamic loading, effects on local failure of fasteners and/or cladding. One way to determine these characteristics is through spectral analysis which is based on the Fourier transform. Yet, to apply Fourier analysis, one needs long records that usually yield broad spectra with no specific peaks. This is due to the fact that these long records consist of intermittent pressure peaks and regions of smaller fluctuations. Consequently, it is not feasible to associate frequencies with pressure peaks. On the other hand, and over the past decade, wavelet analysis has been proposed as a useful tool for detecting coherent structures in atmospheric wind and relating them to observed pressure peaks on structures, in both wind tunnel simulations and full-scale measurements. The reason being that wavelet analysis yields time and scale decomposition of the signal through using localized functions in the physical and Fourier domains. Gurley and Kareem (1997) showed that wavelet analysis can be used to simulate non-stationary wind velocity records. Hajj and Tieleman (1996), Jordan et al. (1997) and Hajj et al. (1998) suggested the use of wavelet analysis to characterize specific events in full-scale velocity measurements and simultaneously measured surface pressure peaks. By stressing the need to quantify intermittent and transient pressure loads and the physical mechanisms responsible for their generation, Pettit et al. (2002) used wavelet analysis to sort detected transient pressure peaks into different classes. Statistical analysis of the resulting classification was then performed to separate the record into a synthesized time series that mimics the intermittent character of the original signal and a remaining signal that can be reasonably modelled as a Gaussian process.

All previous results show clearly the advantages of using wavelet analysis to determine the intermittent characteristics of incident flow and associated transient pressure peaks. Yet, the localized nature of wavelet analysis has its own shortcomings. For instance, the scale and time characterization of a given pressure event can be corrupted by the presence of adjacent events. Moreover, different wavelets can yield different time and scale decompositions. This work aims at answering the question as to whether using different wavelets would yield different characteristics for the pressure peaks or velocity events. A positive answer to this question renders the use of wavelet analysis futile in establishing parameters that can be used in the comparison of wind tunnel and full-scale data. On the other hand, deriving physical parameters that are independent of the analyzing wavelet family strengthens the notion of using wavelet analysis for characterizing surface pressures and wind loads. To achieve the objective of this work, the suitability of the Morlet and Paul wavelets to characterize pressure peaks and velocity events is investigated. The motivation behind using these two wavelets is that the Morlet wavelet is widely used, but its shape may not match well with the characteristic shape of a pressure event. On the other hand, the imaginary part of the Paul wavelet matches spike-like pressure events. Additionally, the time scale of the velocity event that yielded the pressure event is determined and compared with that of the pressure event. In Section 2, the Paul and Morlet wavelets defined and the methodology for defining physical time scales for both wavelets is presented. In Section 3, experimental setup, analysis procedure, and results are presented. Conclusions are drawn in Section 4.

2. The wavelet transform

The continuous wavelet transform allows for local characterization of frequency content in signals or functions. It is defined as

$$W(a,\tau) = \int_{-\infty}^{\infty} f(t)\Psi^*(a, t-\tau)\,\mathrm{d}t, \tag{1}$$

where $f(t)$ is a signal or input function, $\Psi(a,\tau)$ is the wavelet function and the * operator denotes the complex conjugate. There are many different choices for the wavelet function. All of the wavelets in a wavelet family are described by dilated and scaled versions of a mother wavelet. These wavelets and the mother wavelet, $\Psi_m(t)$, are related by

$$\Psi(a,t) = \frac{1}{\sqrt{a}}\,\Psi_m\left(\frac{t}{a}\right), \tag{2}$$

where a is the wavelet scale. The normalization scheme defined in Eq. (2) forces all wavelet scales to have the same energy. Many functions have been used as mother wavelets. A function must satisfy two criteria in order for it to be admissible as a mother wavelet. Expressed in the time domain, the mother wavelet must fluctuate with zero mean and the amplitude must decay to zero rapidly. Equivalently, expressed in the frequency domain, the mother wavelet must have zero DC contribution and a finite bandwidth.

The general Paul wavelet is defined in Farge (1992) as

$$P(m,t) = \mathrm{i}^m(1-\mathrm{i}t)^{-1-m}\Gamma(1+m), \tag{3}$$

where the Gamma function, $\Gamma(m)$, is defined for continuous m as

$$\Gamma(m) = \int_0^\infty t^{m-1}\mathrm{e}^{-t}\,\mathrm{d}t. \tag{4}$$

For integers n, the Gamma function is used as the definition for the factorial as follows:

$$\Gamma(n) = (n-1)! \tag{5}$$

Setting $m = 1$ for the Paul wavelet yields the complex valued mother wavelet which is given by

$$\Psi_m(t) = \frac{\mathrm{i}}{(1-\mathrm{i}t)^2} = \frac{-2t}{(1+t^2)^2} + \mathrm{i}\left(\frac{1-t^2}{(1+t^2)^2}\right) \tag{6}$$

Expressed in real and imaginary components, the scaled Paul wavelet are written as

$$\Psi(a,t-\tau) = -\frac{2a^{5/2}(t-\tau)}{(a^2+(t-\tau)^2)^2} + \mathrm{i}\left(\frac{a^{3/2}(a^2-(t-\tau)^2)}{(a^2+(t-\tau)^2)^2}\right). \tag{7}$$

The Morlet wavelet is obtained by multiplying a complex valued sine and Gaussian functions as follows:

$$\Psi_{\mathrm{Morlet}}(a,t) = \frac{1}{\sqrt{a}}\mathrm{e}^{\mathrm{i}\omega_\psi t/a}\mathrm{e}^{-(t/a)^2/2}. \tag{8}$$

It is important to note that scales, represented by a, from the Morlet and Paul wavelets are not comparable; thus, making a direct comparison between these scales is not useful. In our approach, we compare results from the two different wavelets by relating the scale to a physical (with dimensions) characteristic time, T_c'. For the Paul wavelet, we first choose a nondimensional characteristic time, T_c, as the width of the imaginary part defined by the two positive-to-negative zero crossings. This choice is illustrated in Fig. 1 which shows the real, imaginary, and magnitude of the Paul wavelet along with vertical lines that mark the characteristic time T_c. Using the characteristic time definition of Boashash and Barkat (2001), the relation between the nondimensional characteristic time, T_c as defined here, and the scale a of the Paul wavelet is determined to be $T_c = 2a$. For the Morlet wavelet, the nondimensional characteristic time, T_c is defined as one half period of oscillation as shown in Fig. 2. This definition yields the relation, $T_c = (\pi/\omega_\psi)a$, between the nondimensional characteristic time and the scale, a, of the Morlet wavelet.

The nondimensional characteristic time scales defined above are then converted into physical time scales by relating the nondimensional sampling period of the wavelet, Δt, to the sampling period of the data, $\Delta t'$, which in this case is 0.1 s. Seventeen points were used to sample the mother Paul wavelet with one point at $t = 0$. The sampling is carried out

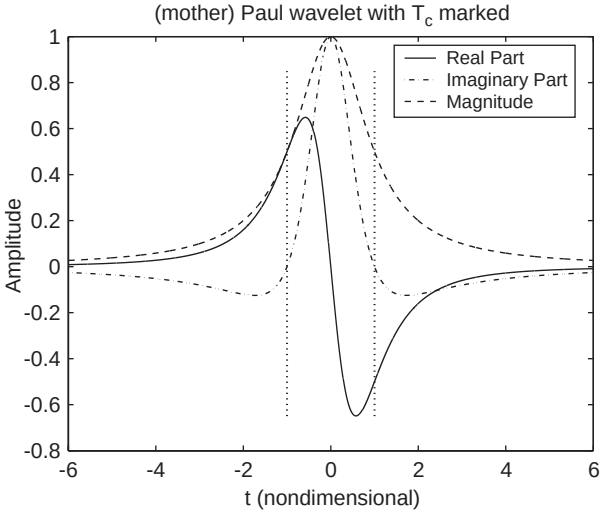

Fig. 1. Real, imaginary, and magnitude of the (mother) Paul wavelet with the characteristic time T_c marked with vertical dotted lines.

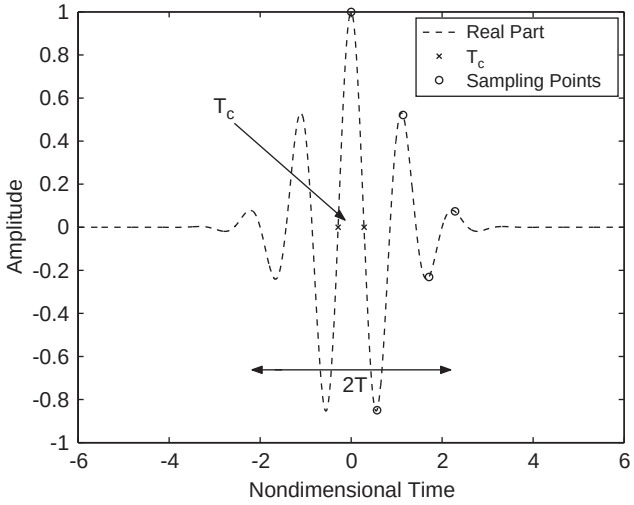

Fig. 2. Real part of the (mother) Morlet wavelet with the sampling time, $2T$, and the characteristic time, T_c, marked.

to $t = 4.429$ where the magnitude of this wavelet is 4.8% of its maximum value. This yielded eight sampling intervals each with a Δt of 0.55363. For the scaled Paul wavelets, a larger number of sampling points was used to maintain the same sampling interval, Δt. The relation between the physical and nondimensional characteristic times for implementing the Paul wavelet is then given by

$$T'_c = \frac{T_c}{\Delta t}\,\Delta t' = \frac{1}{0.55363}\;2\;a\;0.1 \approx 0.361\;a. \tag{9}$$

For the Morlet wavelet, the sampling is carried out over four periods of oscillations by which the amplitude drops to 3.6% of the maximum value. Using nine sampling points for the mother wavelet yields eight sampling intervals each with a Δt of π/ω_ψ. A larger number of sampling points were used for the scaled Morlet wavelets to maintain this same Δt. The relation between the physical and nondimensional characteristic times for implementing the Morlet wavelet is then given by

$$T'_c = \frac{T_c}{\Delta t}\,\Delta t' = 0.1\;a. \tag{10}$$

The relationships presented in Eqs. (9) and (10) allow for the comparison of wavelet-based physical time characteristics of events instead of nondimensional scales, a. This will help in answering the question as to whether different wavelets yield different time and scale decompositions and, thus, establish their suitability for comparing pressure peak characteristics from full-scale and wind tunnel or numerical simulations.

3. Analysis

The data set analyzed in this work is obtained from the Wind Engineering Research Facility Laboratory (WERFL) at Texas Tech University. Fig. 3 shows the dimensions of the WERFL test building and the locations of the pressure taps. Simultaneous velocity and pressure measurements are used in this analysis. The velocity measurements were obtained from a cup-vane anemometer mounted 3.91 m above the ground (same as roof height) and located 46 m from the center of the structure at 35° azimuth angle (see Fig. 3). More details of the measurement setup, techniques and geometry are given in Levitan and Mehta (1991). The u- and v-velocity components are determined from the wind and speed direction as measured by the cup-vane anemometer. The u-component is in the mean wind direction. The v-component is in the direction perpendicular to the mean wind direction in the horizontal plane. The time series of the pressure coefficient at tap 50,501 ($x = 1.52$ m and $y = 0.30$ m) is shown in Fig. 4. The interest is in the pressure peak observed near $t = 513$ s. The choice of this record is based on the wavelet cross-scalogram analysis by Jordan et al. (1997) which showed that this peak had its origin in the v-component of the velocity fluctuations which are shown in Fig. 5. Both time series are a part of the record M15N086 as referred to in the WERFL database.

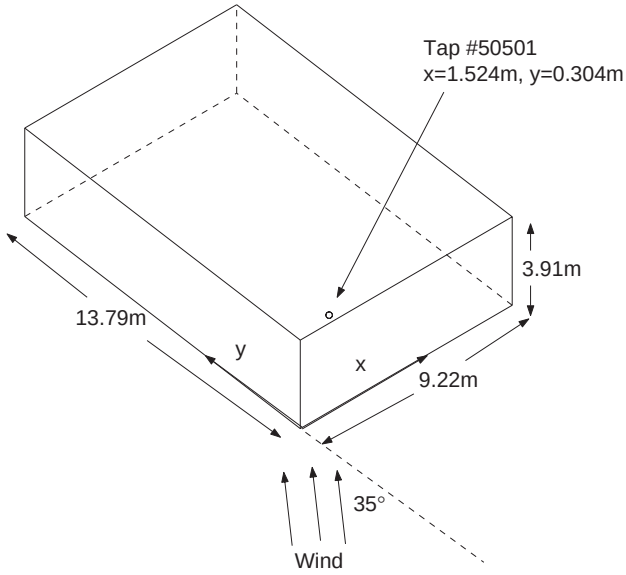

Fig. 3. WERFL test set-up.

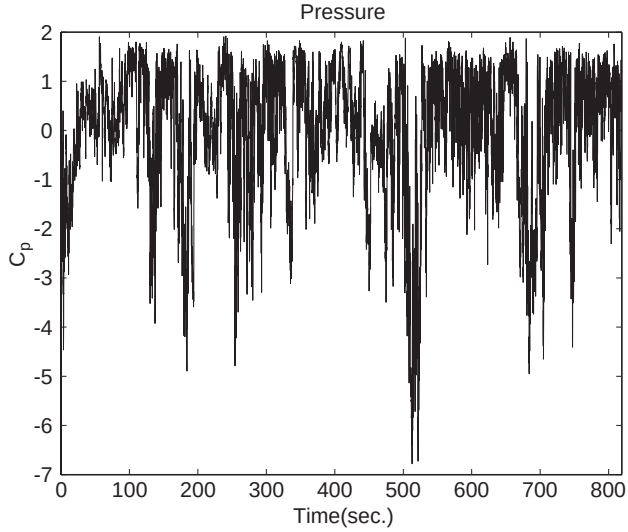

Fig. 4. Pressure record, note the pressure spike at time $t = 513$ s.

3.1. Wavelet coefficients

Contour plots of the magnitude of the wavelet coefficients as obtained from the Morlet and Paul wavelet transforms of the pressure data are shown, respectively, in Figs. 6 and 7. The Morlet wavelet yields two maxima in the magnitude of the wavelet coefficients near the time of the occurrence of the pressure peak ($t = 513$ s). The scales of these maxima are given by $\ln(a) = 3.8$ and 5.8. However, neither maximum is particularly distinct. As for the Paul wavelet, the magnitude of the wavelet coefficients shown in Fig. 7 also exhibit an elongated maximum near time $t = 513$ s. This maximum is spread out over scales between $\ln(a) = 3.9$ and 5.5. Again, this broad range of scales is not useful in characterizing the pressure event. In summary, both the Paul and Morlet wavelet transforms are influenced by adjacent events which cause interference, making it difficult to associate a single scale with the event.

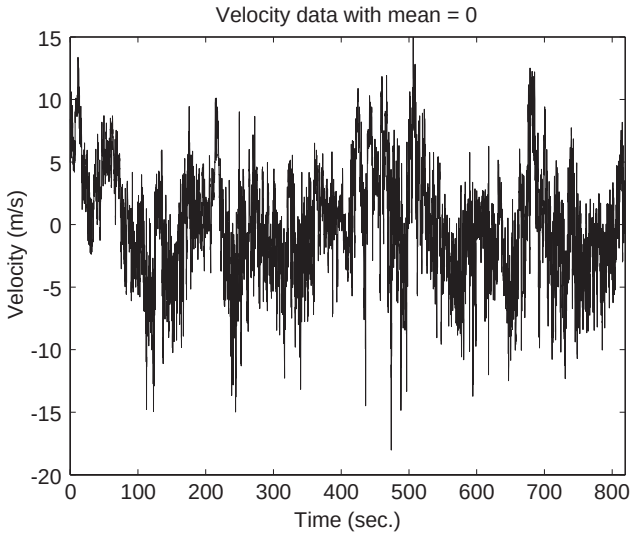

Fig. 5. Unfiltered velocity data; note the zero crossing event at time $t = 503$ s.

Fig. 8 shows the contour plot of the magnitude of the wavelet coefficients obtained with the Morlet wavelet transform of the velocity record. Three local maxima at scales $\ln(a) = 3.2,\ 4.5$, and 5.2 are noted near time $t = 503$ s. The largest maximum is distributed in time over the period between 450 and 520 s over a range of scales given by $\ln(a)$ between 5.2 and 5.5. Thus, the wavelet coefficients do not yield a single scale at the time of interest. A contour plot of the magnitude of the wavelet coefficients obtained applying the Paul wavelet transform to the velocity record is shown in Fig. 9. Again, the results do not show a clear maximum that can be associated with the velocity event. Obviously, the interference from adjacent fluctuations does not allow distinct measurement of the scale of the velocity event.

3.2. Characteristic time scales

In order to isolate the pressure and velocity events from nearby fluctuations, both signals were multiplied by a modified Gaussian function of the form

$$w(t) = \mathrm{e}^{-\pi(t-\mu)^2/\sigma^2} \tag{11}$$

with the σ parameter set to 500 in the v-component and to 175 in the pressure signal. The window was centered at $t = 503$ s in the record of the velocity event and at $t = 513$ s in the record of the pressure event. This difference is based on the zero crossing time in the velocity event and the peak time in the pressure event and is set to account for the convection time of the fluctuation between the measuring point of the velocity fluctuation and the building. The resulting signals for the pressure and velocity fluctuations are shown in Figs. 10 and 11, respectively. For now, the values of σ were decided upon by trial and error to match the widths of each event. The effects of varying σ on the final results will be discussed in Section 3.3.

Contour plots of the magnitude of the wavelet coefficients as obtained from the Morlet and Paul wavelets of the windowed pressure data are shown, respectively, in Figs. 12 and 13. The Morlet wavelet analysis yielded a single peak in Fig. 12 at $a = 221$. Based on Eq. (10), the physical time scale of this peak, T_c', has a value of 22.1 s. The Paul wavelet analysis of the windowed pressure signal, shown in Fig. 13 shows a peak at a scale of $a = 62.8$ which, based on Eq. (9), corresponds to a characteristic time, T_c', of 22.68 s. Obviously, the two different wavelets yield the same characteristic time scale for the pressure event when the data are windowed.

To demonstrate the significance of the estimated characteristic physical time scale, plots of the real part of the scaled Morlet wavelet and the windowed pressure event are overlayed in Fig. 14. Clearly, the low peak of the Morlet wavelet matches very well with the envelope of the pressure peaks. Fig. 15 shows an overlay plot of the imaginary part of the scaled ($a = 62.8$) Paul wavelet and the windowed pressure data. Again, there is clear matching between the imaginary part of the wavelet and the physical event. It must also be noted that the Paul wavelet captures the envelope of the event and dies out as the event dies out. The tails of the wavelet contribute very little information to the wavelet coefficients

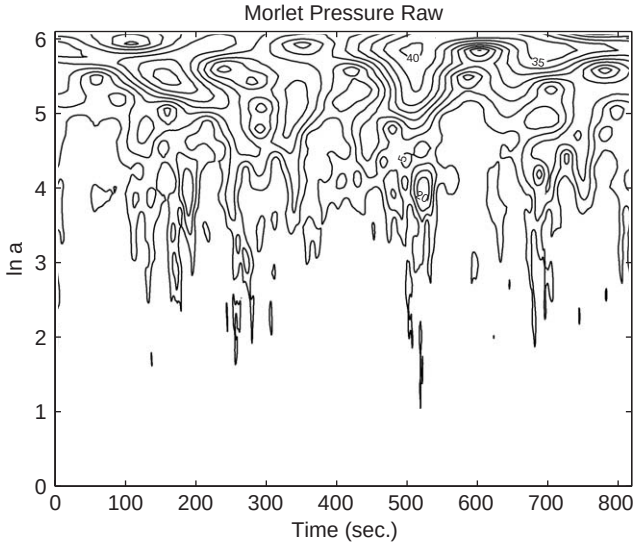

Fig. 6. Morlet wavelet transform of the pressure data. The pressure event is visible at time $t = 513$ s but the largest magnitude scales are distributed over approximately 75 s.

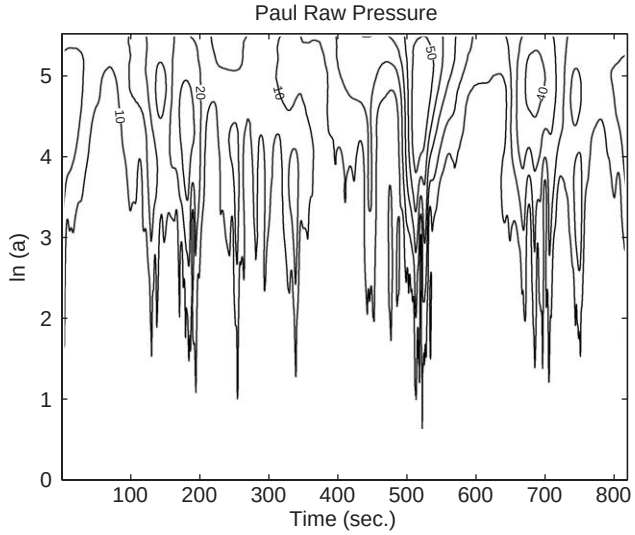

Fig. 7. Paul wavelet transform of the pressure data. The pressure event is visible but many events surround it, affecting the measured scale of the event.

while the bulk of the information that is picked up is due exclusively to the pressure event. In both cases, the characteristic time scale presents a measure of the duration of the pressure event.

Contour plots of the magnitude of the wavelet coefficients obtained with Morlet and Paul wavelet transforms of the windowed velocity signal are shown in Figs. 16 and 17, respectively. A peak at scale $a = 221$ is noted in Fig. 16. This peak is localized in both time and scale and yields a physical characteristic time of 22.1 s. The peak in Fig. 17 which is obtained with the Paul wavelet transform takes place at a scale given by $a = 55$. This peak is also highly localized in time and scale. The corresponding physical characteristic time, T_c', is calculated to be 19.86 s. Again, it is of interest to note that the analyses with *both* wavelets yield the same physical characteristic time. Additionally, this time is close to the characteristic time of the pressure event. This indicates that a major variation in the incoming flow was responsible for the peak in the pressure event.

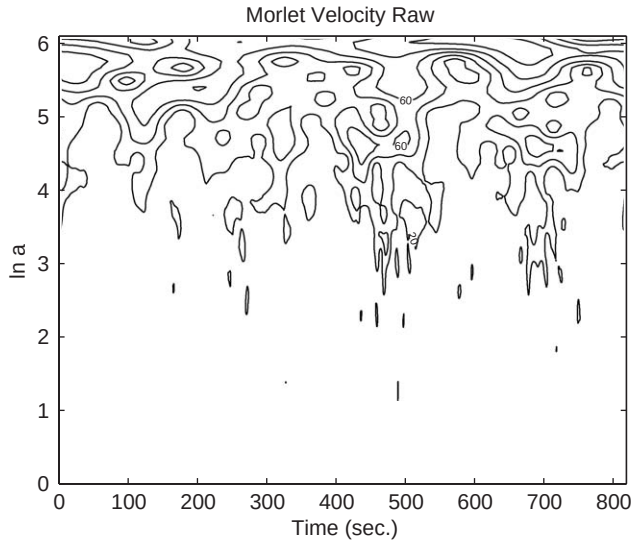

Fig. 8. Morlet wavelet transform of the velocity record. The velocity event is not distinct.

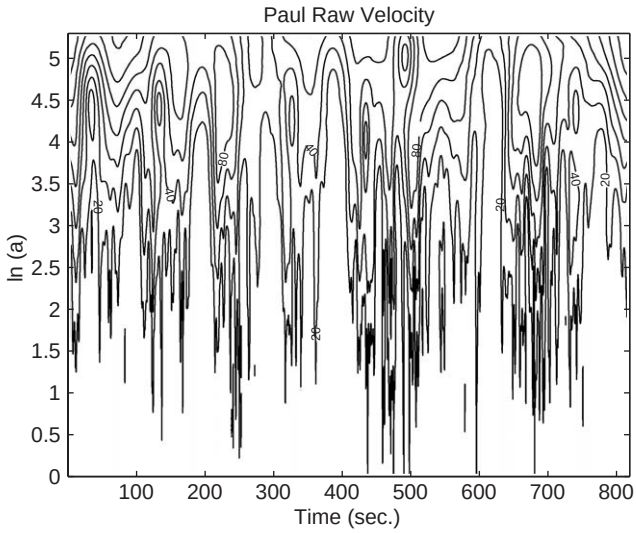

Fig. 9. Paul wavelet transform of the velocity record. The velocity event stands out, but the peak scale of $a = 51$ is not characteristic of the event; more isolation is needed.

Overlayed plots of the real part of the Morlet wavelet and the windowed velocity signal are shown in Fig. 18. Again, the peak oscillation of the wavelet matches well with the velocity event. It should be noted here that the smaller oscillations of the Morlet wavelet extend beyond the event and, in doing so, would have contributed to $|W|$ if windowing was not applied. Even though the Morlet wavelet extends beyond the event, the characteristic time of half a period matches reasonably well with the event. The extra oscillations of the Morlet wavelet correspond to zeros in the signal as a result of windowing. Fig. 19 shows a plot of the real part of the scaled Paul wavelet and the windowed signal. The real part of the Paul wavelet matches the velocity event closely and dies out as the event dies out. Clearly, the information being picked up by the Paul wavelet is restricted to the event scale, so there is no extra information influencing the wavelet transform. The results presented above suggest that by isolating the event, the wavelet will be forced to measure the event scale.

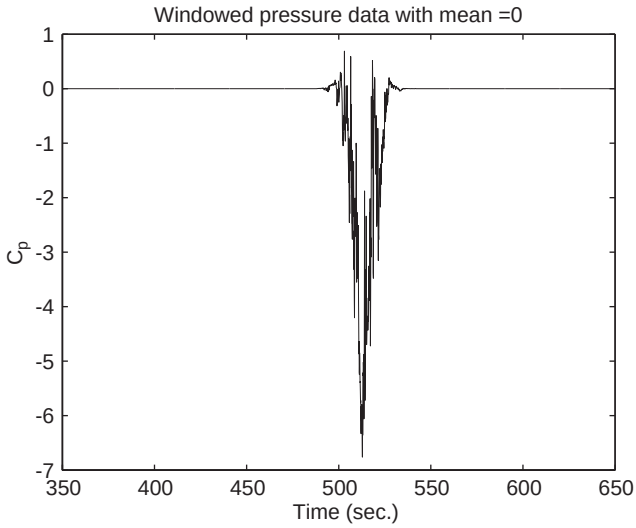

Fig. 10. Windowed pressure data. The pressure event has a characteristic spike-like structure.

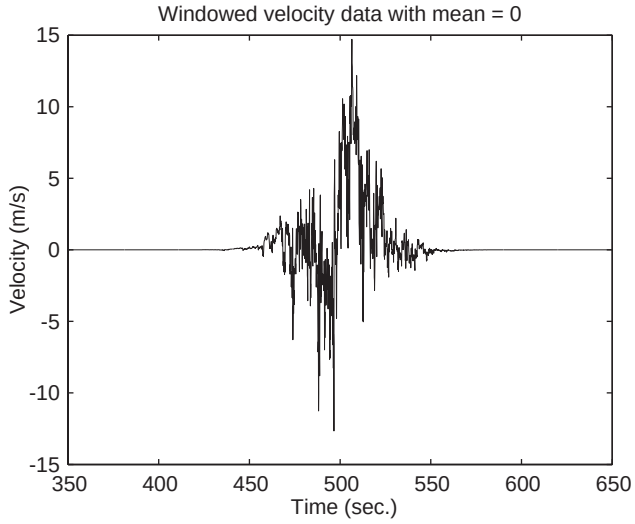

Fig. 11. Windowed velocity data, the zero crossing event has been isolated.

3.3. *Effects of windowing*

The wavelet analysis of the pressure peak and velocity events yield distributed regions of large-magnitude wavelet coefficients for both the Paul and Morlet wavelets. Consequently, it is very difficult to associate these peaks or events with a specific scale. The reason being that the tails of the wavelets pick up contributions from the fluctuations near the event of interest.

It must be noted that decreasing the window width, by decreasing the value of σ, would cause the wavelet to pick up the characteristic time of the window instead of the event. On the other hand, increasing the window size leads to interference from adjacent events. To clarify these points, plots that show variations in characteristic time as a function of window size are shown in Figs. 20 and 21. Fig. 20 shows the dependence of the characteristic time in the pressure signal on the window width using the Paul and Morlet wavelets. The window was varied from $\sigma = 20$ to 1600 and applied at $t = 513$ s. The time scale as measured by the Morlet wavelet increases with the window size and levels off around 32 s. While the time scale measured by the Paul wavelet increases to around 35 s.

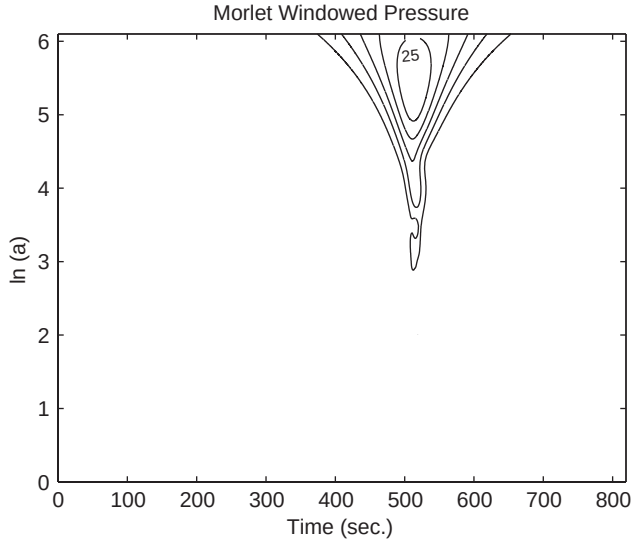

Fig. 12. Wavelet coefficients, $|W|$, of the Morlet wavelet transform of the windowed pressure data shown in Fig. 10. The largest magnitude appears at the scale $a = 221$ which corresponds to a characteristic time of $T_c' = 22.1$ s.

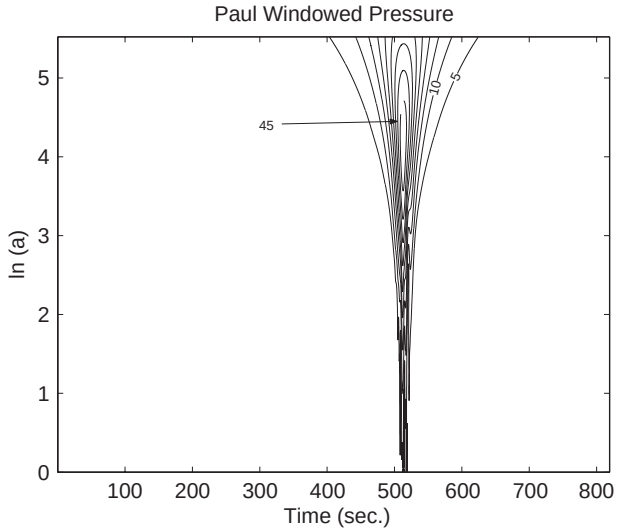

Fig. 13. Wavelet coefficients, $|W|$, for the Paul wavelet transform of the windowed pressure data shown in Fig. 10. The largest magnitude appears at the scale $a = 62.8$ which corresponds to a characteristic time of $T_c' = 22.68$ s.

Fig. 21 shows a comparison of the Morlet wavelet and the Paul wavelet as a function of window width using the velocity data. The window was varied from $\sigma = 20$ to 1600. The characteristic time measured by the Morlet wavelet varies over the range of windows and levels out to a constant value of about 25 s. The largest time scale measured by the Paul wavelet was about 20 s and stayed roughly constant for window widths above $\sigma = 175$. Below $\sigma = 175$ both wavelets picked up the window width rather than the event. It should be stressed how the two different two wavelets give the same characteristic time for events *only* when the window width correctly isolates the events. For window sizes of $\sigma > 500$ in the velocity signal and window sizes of $\sigma > 175$ in the pressure signal, the two wavelets give different estimates of the characteristic time scales.

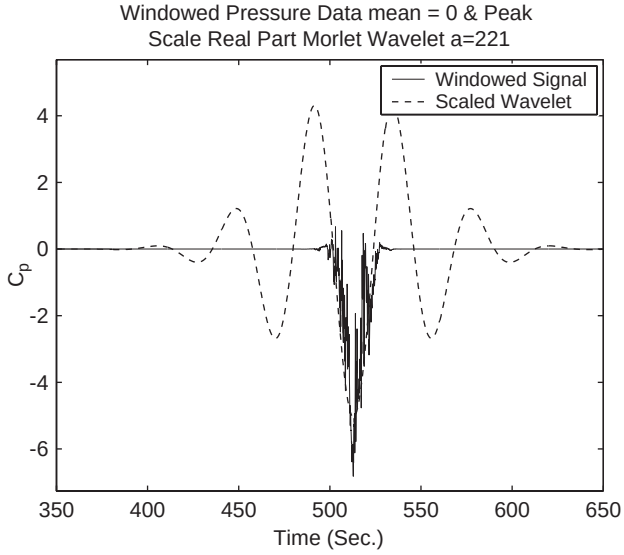

Fig. 14. The scaled Morlet wavelet ($a = 221$ and $T_c' = 22.1$ s) plotted over the pressure spike.

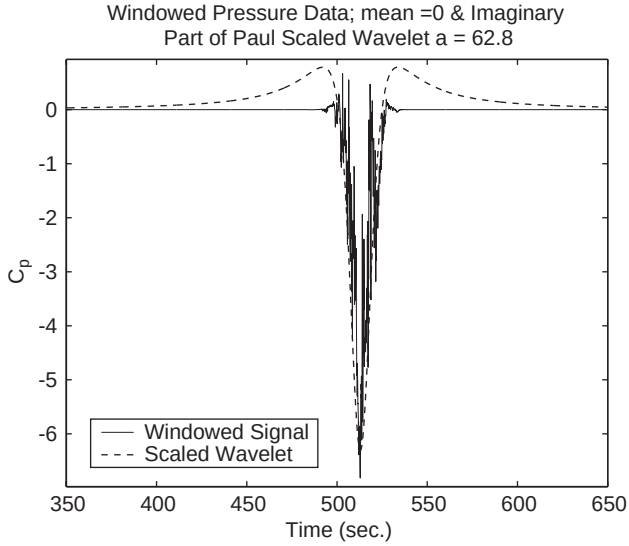

Fig. 15. The scaled Paul wavelet ($a = 62.8$ and $T_c' = 22.68$ s) plotted over the pressure spike.

Based on the above results, a consistent analysis procedure for determining a characteristic time scale for pressure peaks and velocity events is presented. This procedure was determined from several analysis trials on wind tunnel data that made use of both Morlet and Paul wavelets, as detailed by Chabalko (2001). First, the mean and standard deviation of the time series are calculated. Second, the signal is conditionally sampled so that values smaller in magnitude than the mean minus three standard deviations are set equal to zero. Values larger in magnitude are then shifted up by the mean plus three standard deviations. The start and end of the peak are then identified by the zero end points. Once a peak is identified, it is multiplied by a window that is centered at the peak minimum and that has a width that is 30% wider than the peak itself. The window width is defined by the 95% amplitude reduction. The characteristic time scale is then determined by applying wavelet analysis to the windowed peak.

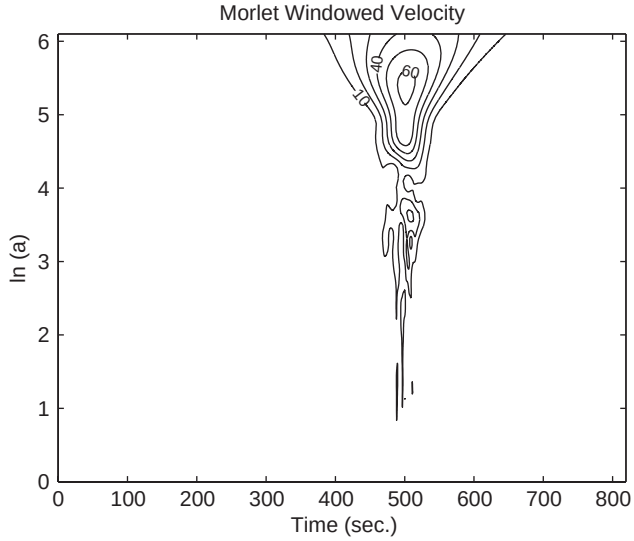

Fig. 16. Wavelet coefficients, $|W|$, of the Morlet wavelet transform of the windowed velocity data shown in Fig. 11. The coefficients are compactly distributed in time near the event. The peak scale is $a = 221$ which corresponds to a characteristic time of $T_c' = 22.1$ s.

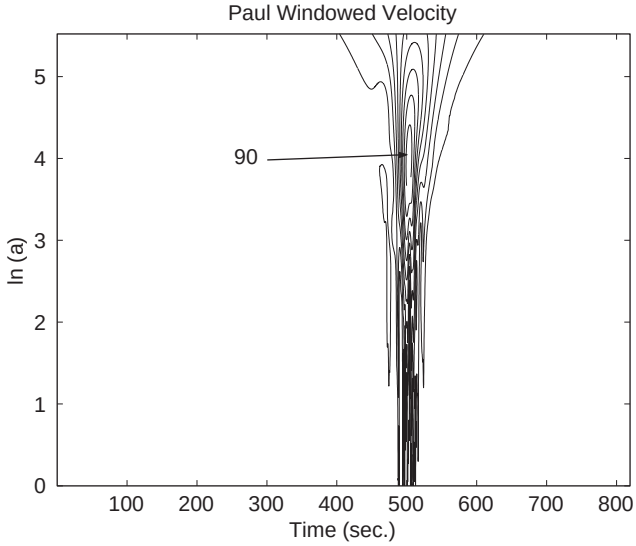

Fig. 17. Wavelet coefficients, $|W|$, for the Paul wavelet transform of the windowed velocity data shown in Fig. 11. The peak scales are localized in time near the event. The peak scale, $a = 55$, corresponds to a characteristic time, $T_c' = 19.85$ s.

4. Conclusions

In this work, physical time scales of a pressure peak and a highly correlated velocity event are determined from wavelet analysis with two different wavelet functions, namely the Paul and Morlet wavelets. The results show that, by isolating the peaks or events with a modified Gaussian window prior to applying the wavelet transform, the dependence of the estimated time scale on the type of wavelet function is reduced. The effects of varying the window width show

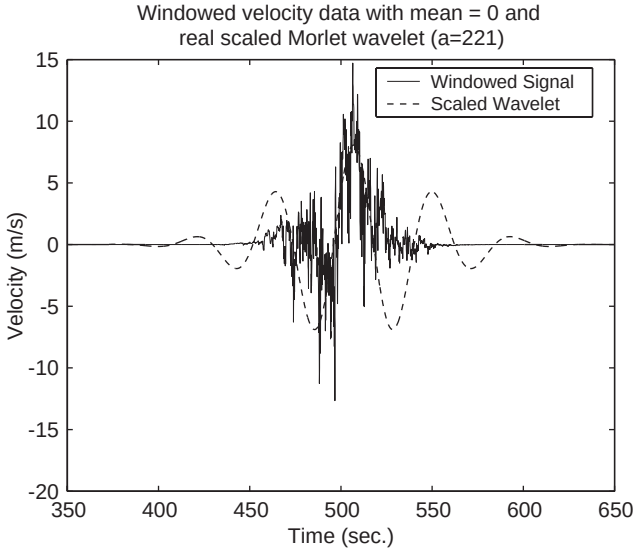

Fig. 18. The scaled Morlet wavelet ($a = 221$ and $T'_c = 22.1$ s) plotted over the velocity event.

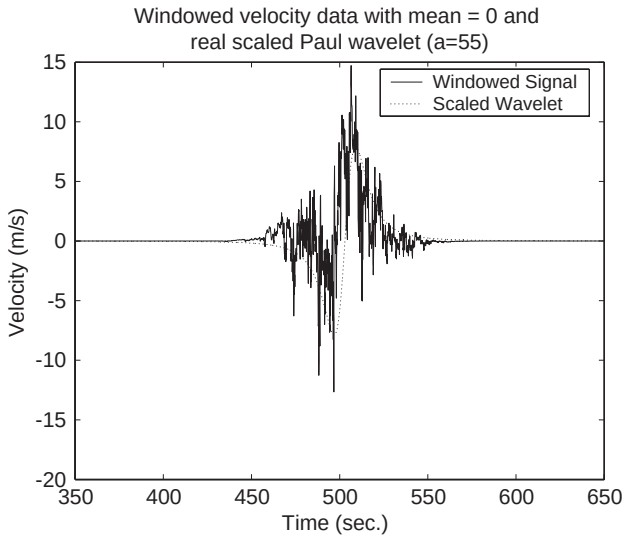

Fig. 19. The scaled Paul wavelet ($a = 55$ and $T'_c = 19.85$ s) plotted over the velocity event.

that the two different wavelet functions give the same characteristic time, only when the window width is neither too small to pick up the characteristic time of the window instead of that of the event nor too large to be affected by interference from adjacent events. The time scales of the pressure peak and the velocity event for the case considered here are estimated to be about the same, indicating that the major contributing factor to the pressure peak lies in the variation of the incoming flow. These results show that pressure peaks and associated velocity events characteristics are independent of the type of wavelet used. Consequently, wavelet analysis can be used for the purpose of comparing characteristics of pressure peaks from wind tunnel and numerical simulations and full-scale measurements.

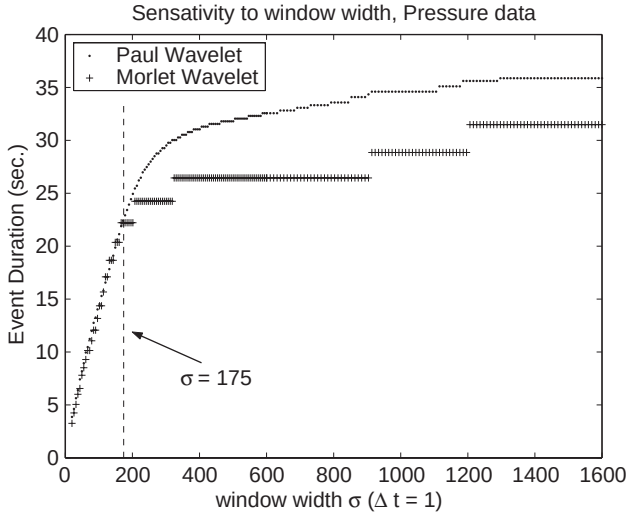

Fig. 20. Variations in characteristic time, T_c', of pressure signal with window width.

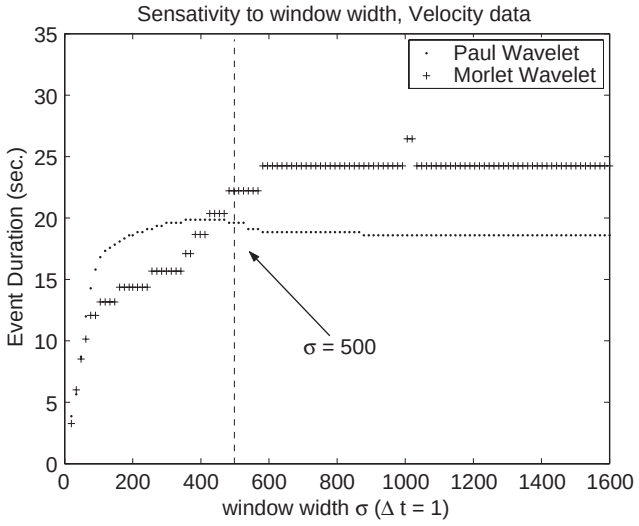

Fig. 21. Variation in characteristic time, T_c', of velocity fluctuation with window width.

Acknowledgements

This work is supported by the National Institute of Standards and Technology through the Hurricane Loss Reduction Consortium, Clemson University under award number 70NANB2H0159. The authors wish to also thank Dr K. Mehta and the staff of WERFL at Texas Tech for providing the data.

References

Boashash, B., Barkat, B., 2001. Introduction to time frequency analysis. In: Lokenath Debnath (Ed.), Wavelet Transforms and Time Frequency Signal Analysis. Birkhauser, Basel, pp. 321–380 (Chapter 11).

Chabalko, C.C., 2001. Comparison of Paul and Morlet wavelets for measuring the characteristic scale of peak pressure events on low-rise structures. M.Sc. Thesis, Virginia Tech.

Farge, M., 1992. Wavelet transforms and their applications to turbulence. Annual Review of Fluid Mechanics 24, 395–457.

Gurley, K., Kareem, A., 1997. Analysis interpretation modeling and simulation of unsteady pressure data. Journal Wind Engineering and Industrial Aerodynamics 69–71, 657–669.

Hajj, M.R., Tieleman, H.W., 1996. Application of wavelet analysis to incident wind in relevance to wind loads on low-rise structures. ASME Journal of Fluids Engineering 118, 874–876.

Hajj, M.R., Jordan, D., Tieleman, H.W., 1998. Analysis of atmospheric wind and pressures on a low rise building. Journal of Fluids and Structures 12, 537–547.

Jordan, D.A., Hajj, M.R., Tieleman, H.W., 1997. Wavelet analysis of the relation between atmospheric wind and pressure fluctuations on a low-rise building. Journal Wind Engineering and Industrial Aerodynamics 69–71, 647–655.

Levitan, M.L., Mehta, K.C., 1991. Texas Tech field experiments for wind loads; Part I: building and pressure measurement system. Journal Wind Engineering and Industrial Aerodynamics 41–44, 1569–1576.

Pettit, C.L., Jones, N.P., Ghanem, R., 2002. Detection and simulation of roof-corner pressure transients. Journal Wind Engineering and Industrial Aerodynamics 90, 171–200.